N84 27265

SPECTRASAT: A CONCEPT FOR THE COLLECTION OF GLOBAL DIRECTIONAL WAVE SPECTRA

Robert C. Beal
The Johns Hopkins University
Applied Physics Laboratory
Johns Hopkins Road
Laurel, Maryland 20707

ABSTRACT

The synthetic aperture radar (SAR) imagery from Seasat revealed a rich tapestry of backscatter patterns from the surface of the ocean. Although still far from being fully understood, these patterns occurred on nearly all spatial scales accessible to the SAR, that is, from its spatial resolution of 25 m to its full swath width of 100 km. Furthermore, the backscatter signatures appear to reveal a large variety of atmospheric and oceanic processes that occur above, at, and below the ocean surface. Proper interpretation of these signatures of varying scales with respect to their underlying geophysical causes is a major objective of SAR ocean research. Even now, however, it is clear that SAR offers a unique means to monitor wind and waves over global scales. A properly designed, configured, and complimented orbiting SAR system should yield substantial improvements in operational forecasts vital to marine activities. Since wind and wave information can be optimally extracted in the spectral domain, the name "Spectrasat" is proposed for this global collection scheme.

1. GEOPHYSICAL SIGNATURES IN SAR OCEAN IMAGERY

1.1 Background

Any geophysical process which directly or indirectly influences the short 30 cm waves on the ocean surface will produce a signature in SAR imagery (Beal, DeLeonibus, and Katz, 1981; Fu and Holt, 1982). Figure 1 is a particularly vivid illustration of the variety of signatures evident in a single 2 minute SAR pass (pass 1339, 28 September 1978). Some of these effects are easily visible in the spatial domain; others are much more obvious in the spectral domain. Moreover, some signatures are instantaneous expressions of the wind field, while others are the results of winds occurring many days previously and thousands of kilometers distant.

1.2 A Seasat Data Base

Figure 1a, derived from an examination of Seasat scatterometer wind fields over a several day period, shows the spatial and temporal locations of two separate storm systems as they evolved during the days just prior to SAR pass 1339. Both of these storms spawned wave systems eminating from their centers, and propagating generally toward the west, i.e., toward the SAR overpass region (Beal, Monaldo, and Tilley, 1983). The southernmost "primary" storm was the more intense of the two, and reached peak winds in excess of 20 m/s and peak

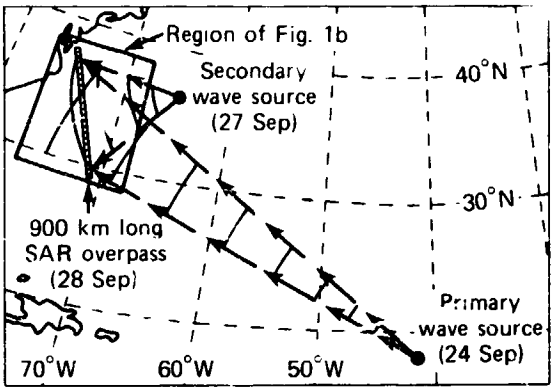

Fig. 1a Sources of wave energy in the North Atlantic, 28 Sep, 1978.

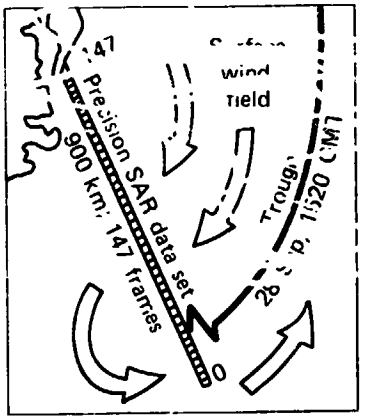

Fig. 1b Location of 900 km long SAR pass, divided into 147 6.4 km squares.

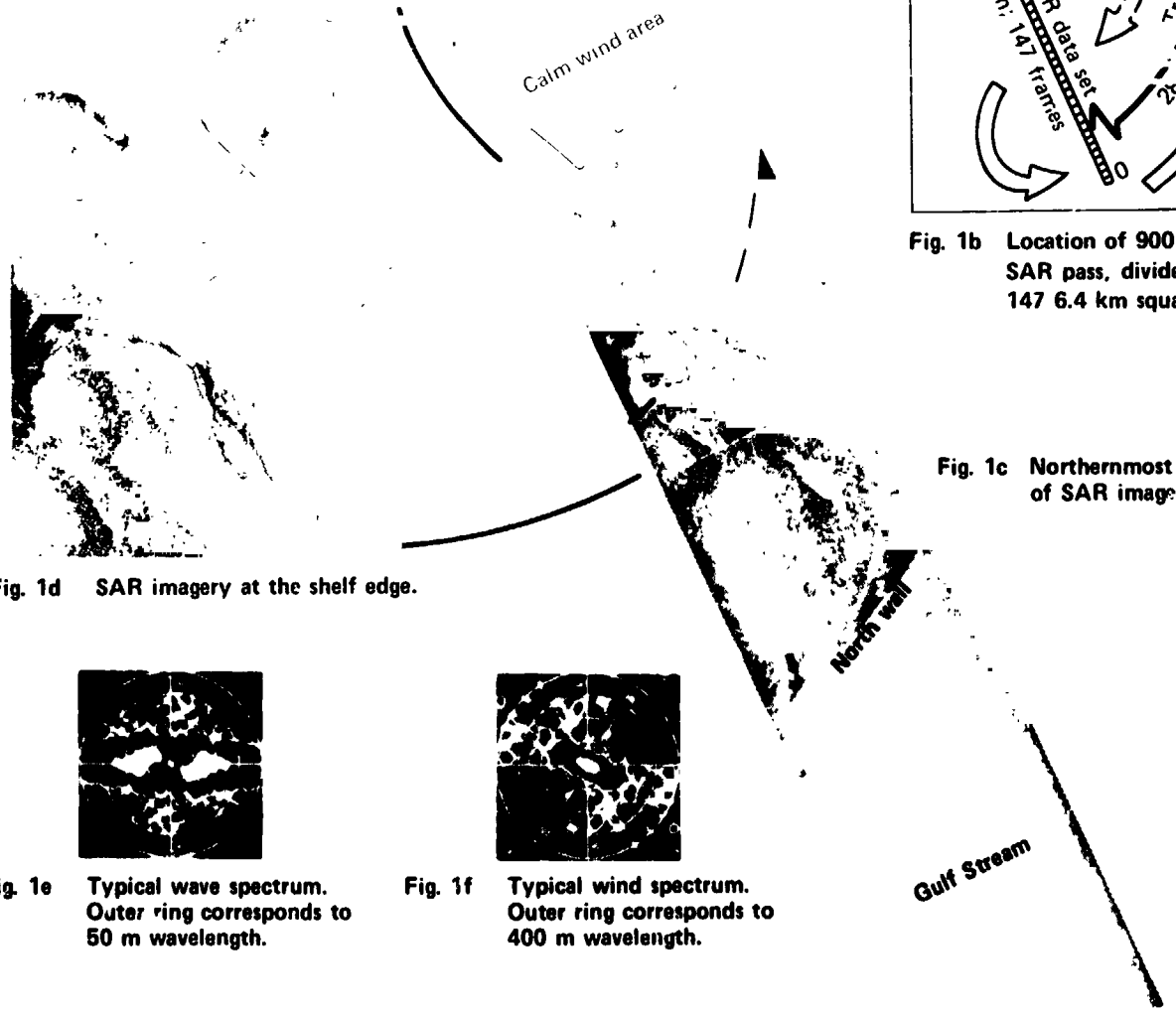

Fig. 1c Northernmost 300 km of SAR imagery.

Fig. 1d SAR imagery at the shelf edge.

Fig. 1e Typical wave spectrum. Outer ring corresponds to 50 m wavelength.

Fig. 1f Typical wind spectrum. Outer ring corresponds to 400 m wavelength.

Fig. 1 Various types of signatures in SAR imagery.

(significant) wave heights of about 6 m (as measured by the Seasat altimeter) before subsiding. As this wave system approached the East Coast of the United States, the average wavelength was ~200 m, and the wave height had diminished to about 0.75 m.

Meanwhile, also from an examination of previous scatterometer wind fields, a somewhat weaker, but spatially and temporally more proximate "secondary" storm had developed about 1000 km from the impending 900 km long SAR overpass. This wind field barely reached 15 m/s, and spawned waves of height 2 to 3 meters. Since the secondary wave source was so much closer to the SAR overpass, however, the resulting wave field experienced rapid spatial evolution.

Figure 1b illustrates the area in the immediate vicinity of the SAR overpass, which occurred as waves from both sources were propagating through the region. Figure 1c shows the northern third of the SAR overpass. The displayed imagery is only 40 km wide by about 300 km long, and was collected in less than 1 minute, but contains much information on wind, waves, and currents.

1.3 Surface Current Boundaries

The Gulf Stream North Wall, as well as a number of mesoscale eddies, are apparent as quasi-linear features just above the center of the imagery. These small eddies are shown in greater detail in Figure 1d. Current shear boundaries apparently excite the 30 cm waves to provide a high contrast signature in the SAR imagery, particularly at lower (2-5 m/s) wind speeds.

1.4 Surface Wind Magnitude

The overall brightness of the SAR image is generally correlated with the amplitude of the 30 cm surface waves, which in turn responds directly to the local wind. This relationship is most clearly evident at very low wind speeds, where the 30 cm waves are effectively extinguished. Although the amplitude of these waves may not continue to increase indefinitely with wind magnitude, there is good evidence (from simultaneous aircraft and scatterometer measurements) that the local average brightness (or radar backscatter) of Figure 1c is strongly correlated with surface wind magnitude up to 13 m/s. Figure 2 shows the correlation between scatterometer-deduced winds and SAR backscatter over an entire 900 km pass length, of which Figure 1c represents the northern third.

1.5 Surface Wave Fields

For long (50-500 m) surface waves, there is an apparent periodic spatial modulation of the local wind-generated 30 cm waves. The modulation may be much less than the noise on the scale of a single 25 m resolution element, but the spatial spectrum of the wave field is generally well-behaved and homogeneous over tens and even hundreds of kilometers. Extensive averaging over both wavenumber and space, therefore, can reduce a very noisy background by as much as a factor of 20 or 30, revealing extremely subtle modulations of only a few percent. For example, Figure 1e illustrates the extensively

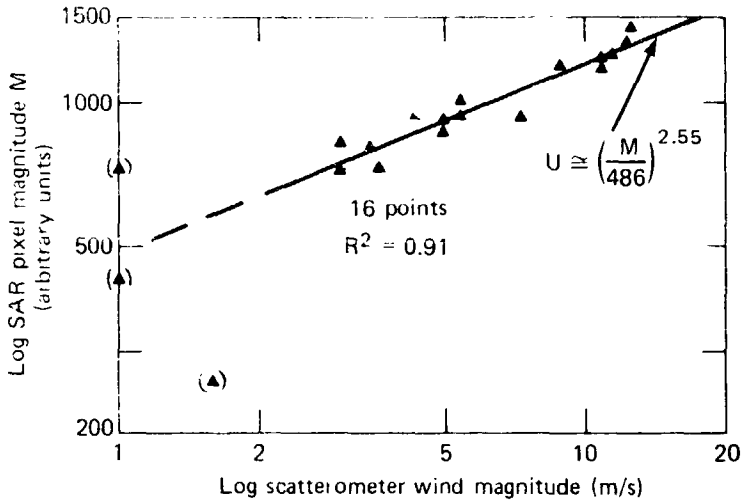

Fig. 2 SAR backscatter magnitude versus scatterometer winds.

spatially and spectrally smoothed spectrum of a portion of Figure 1d. The noise has been reduced to the point where the primary (200 m wavelength) and secondary (100 m wavelength) systems are clearly distinguishable, even though the significant waveheight of each system was under 1 m in this portion of the pass. With appropriate (and, in the future, perhaps adaptable) filtering, the spatial evolution of the dominant vector wavenumber can be tracked with mean residuals of only a few percent. Figure 3a shows the result of near-optimal tracking of the primary wavenumber over 900 km, clearly showing deep-water dispersion, refraction in the Gulf Stream, and shallow water wavelength shortening. Moreover, Figure 3b shows subtle perturbations of the wavenumber in shallow water which reveal the presence of subsurface mounts and depressions. The angular evolution of the wavenumber accurately locates the (previous) position of the wave generation sources.

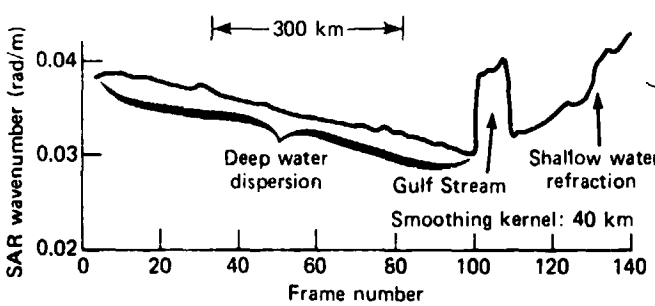

Fig. 3a Entire 900 km pass

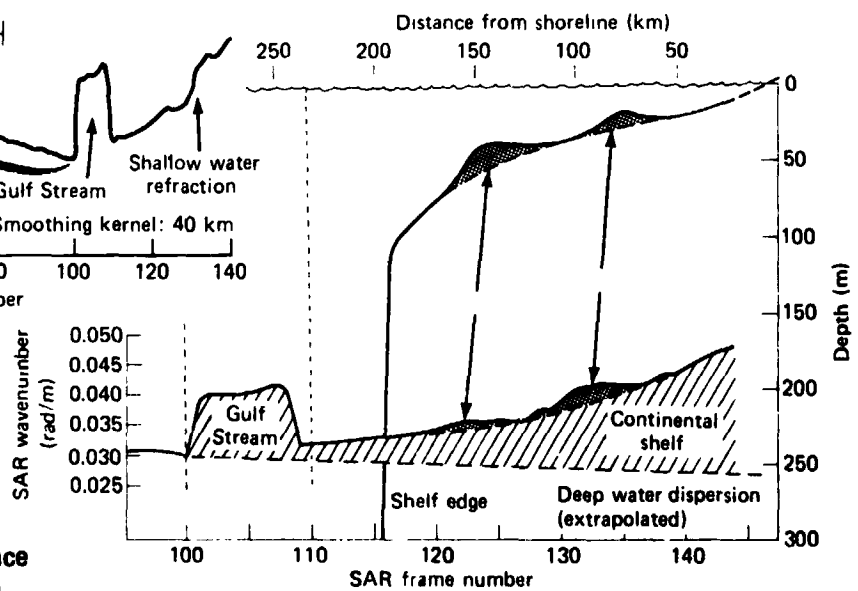

Fig. 3b Northernmost 300 km

Fig. 3 SAR wavenumber refraction in the presence of currents and bottom topography for pass 1339.

1.6 Surface Wind Direction

The horizontal wind field at the surface of the ocean is neither temporally nor spatially homogeneous. In particular, as the horizontal component of the wind stresses the surface, it produces large streaks of higher backscatter, aligned with the local wind direction, and having spatial scales of a few hundred meters to a few km. At the higher wind speeds, and when the water surface temperature exceeds that of the air, elongated atmospheric convection cells can be established, with their long axes aligned with the wind. Both phenomena exhibit asymmetric spatial spectra which can reveal the direction of the local wind, when properly processed. A typical example of such a wind direction signature is illustrated by the asymmetric shape of the spectral energy bundle about the origin of Figure 1e, or its higher wavenumber resolution equivalent in Figure 1f. In both cases, the minor axis is closely aligned with the best estimate of the local wind direction from the scatterometer. Figure 4 summarizes the accuracy of this technique for wind direction estimation with respect to scatterometer estimates. On this pass at least, the residual directional deviations from a smoothed estimate of the local wind field are approximately equal when determined from either the scatterometer or the SAR. Moreover, the SAR may be yielding an estimate of the fine scale spatial spectrum of the wind field, which could be useful in the understanding of scatterometer wind field estimates.

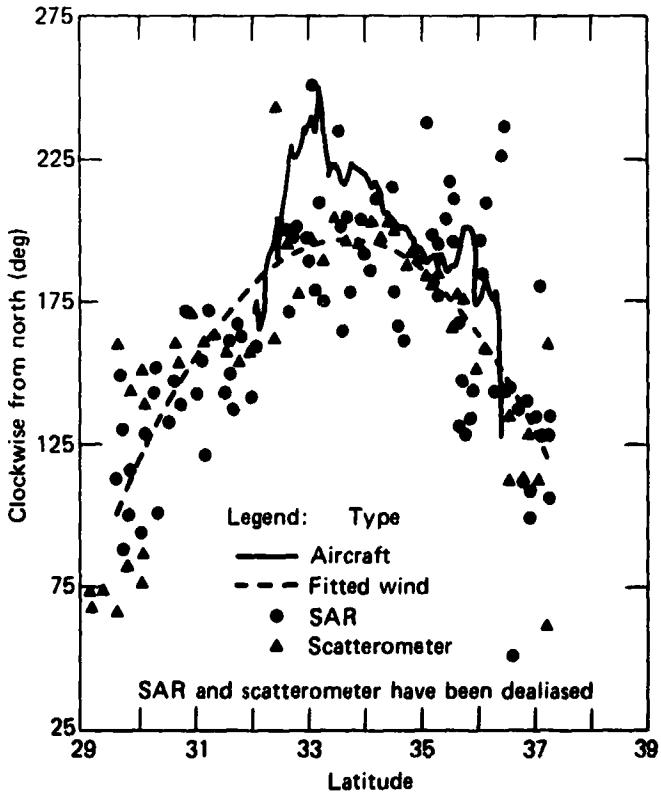

rms residuals
with respect to
smoothed estimate:

scatterometer	22.5°
SAR	24.5°

Fig. 4 Various wind direction estimates.

2. SOME PRACTICAL PROBLEMS AND CAVEATS

2.1 General Comments

As the above evidence clearly demonstrates, spaceborne SAR possesses a fascinating ability to reveal current boundaries, spatially evolving directional wave spectra, and even the magnitude and direction of the local wind field. Prior to Seasat, there existed no satisfactory theory which would have predicted these results; indeed, even now the experimental evidence is forcing the theoretical advances. In spite of these encouraging results, however, we must still admit to a number of fundamental limitations in our present state of knowledge.

2.2 Doppler Smear

One of the more controversial aspects of SAR concerns its limitations for imaging moving ocean waves (see, for example, the Journal of Geophysical Research Special Issue on MARSEN, 1983). Being a Doppler measuring device which implicitly assumes a stationary target for precise focusing and location, a randomly moving ocean wave presents a particular challenge. In view of the results shown in Figure 3, however, this limitation is not necessarily devastating. The Doppler motion is most severe for short waves travelling in the direction of the spacecraft; these waves are effectively smeared, or filtered, in the SAR spectrum. The effect can be seen quite clearly in Figure 1e as an absence of energy at the higher spatial wavenumbers. Fortunately, in the pass discussed above, both the primary and secondary wave systems are within the "azimuth passband" of the SAR.

In future SAR systems, the only practical way of increasing the azimuth passband (which is narrowest at high sea states) is to reduce the altitude of the spacecraft. A factor of four reduction over the Seasat altitude of 800 km may be feasible with active drag compensation; such a reduction could effectively eliminate the azimuth smear problem. The upcoming Shuttle Imaging Radar experiment (SIR-B) will offer an excellent opportunity to check this hypothesis.

2.3 Spatial and Temporal Coverage

Data rates from spaceborne SAR can be many hundreds of megabits per second; the problem is particularly aggravated by requirements for wide swaths and high resolution. Construction of a synthetic aperture in real time, on board the satellite, has been consequently frustrated by both the overwhelming data rates and the required size of the processing and storage arrays. Yet, for both wind and wave spectra, especially in deep water, the actual information rate is trivial - perhaps a kilobit per second. Moreover, there is good evidence that reliable wind and wave spectra can be generated over spatial dimensions of under 10 km. One might therefore envision a SAR system sampling the global wave field very much as the Seasat scatterometer sampled the global wind field, that is, with 500 km equatorial spacings between tracks, and repetitive coverage every three days. Although such coverage is less than ideal for detailed storm tracking, it is at least consistent with the scatterometer coverage,

and is probably the best that can be expected with a single satellite.

2.4 Auxiliary Data Sources

Probably the primary rationale for orbiting a narrow swath SAR would be for the collection of global wave spectra. By themselves, these spectra would be of little value, but as a supplement and periodic update to a global wind-wave forecast model, the impact of actual measurements of directional spectra could be revolutionary. For example, present wave generation models in operation around the world are in gross disagreement with respect to the directional properties of waves generated from even the simplest wind fields (c.f., the Sea Wave Modelling Project "SWAMP", in press). There are no good data on the large scale directional evolution of wind-driven waves, and therefore no valid criteria for the acceptance or rejection of particular models.

This dilemma could be solved if there existed a comprehensive set of evolving winds, together with their resultant evolving (directional) waves. The SAR, although capable of precisely tracking the magnitude and direction of the dominant wavenumber, has generally proven elusive with respect to an estimate of the total wave energy. The problem is aggravated both by the Doppler smear effect present in existing data, and by the absence of accurate and comprehensive independent estimates of wave energy. Concurrent altimeter estimates of significant wave height will probably be of value in calibrating the SAR relative directional spectra in an operational configuration.

3. SPECTRASAT: ITS MAJOR CHARACTERISTICS

3.1 Motivation for Proposal

"Spectrasat" is an initial attempt to define the major properties of a SAR satellite specifically designed for the global collection of ocean wave spectra. Although the initial version of Spectrasat can be quite explicit, many of the design parameters are tentative, pending an analysis of SIR-B results in 1985 and 1986. Nevertheless, it is important even now to define a "strawman" version of Spectrasat, both to stimulate debate, and to aid in the design and analysis of future SAR ocean experiments.

3.2 General Characteristics

Spectrasat should be a low (200-250 km) altitude satellite, with active drag compensation. The instantaneous ground swath need be sufficient only for a statistically reliable transform, probably of order 10 km or less. This small swath will allow a greatly reduced (with respect to Seasat) along-track antenna dimension, probably only 1 to 2 m. The potentially overwhelming data rate problem is consequently alleviated, not only by the reduction in swath, but also possibly by sparse sampling of the spectra, similar to the scheme planned for the European Remote Sensing Satellite ERS-1 in its sampled Wave Mode. Global sampling strategies will depend mainly on the scale size of storms in the open ocean, and on whether oceanographic significance can be attached to the observed fine scale (<50 km) evolution of the dominant wave vector.

An adaptive sampling strategy, built around an onboard buffer storage and electronically steerable antenna beams, could allow increased sampling in the vicinity of developing storms, and a commensurate decrease in the more benign regions. Spectrasat, or an experimental precursor, should operate in the presence of NROSS (Navy Remote Ocean Satellite System), ERS-1, or some similar global wind measuring system. so that its directional wave spectra may be interpreted in the context of a simultaneously developing global wave forecast model. Indeed, the ultimate test of Spectrasat will be to significantly improve the wave forecast model through the addition of actual directional wave measurements. Figure 5 illustrates the basic geometry of the proposed satellite.

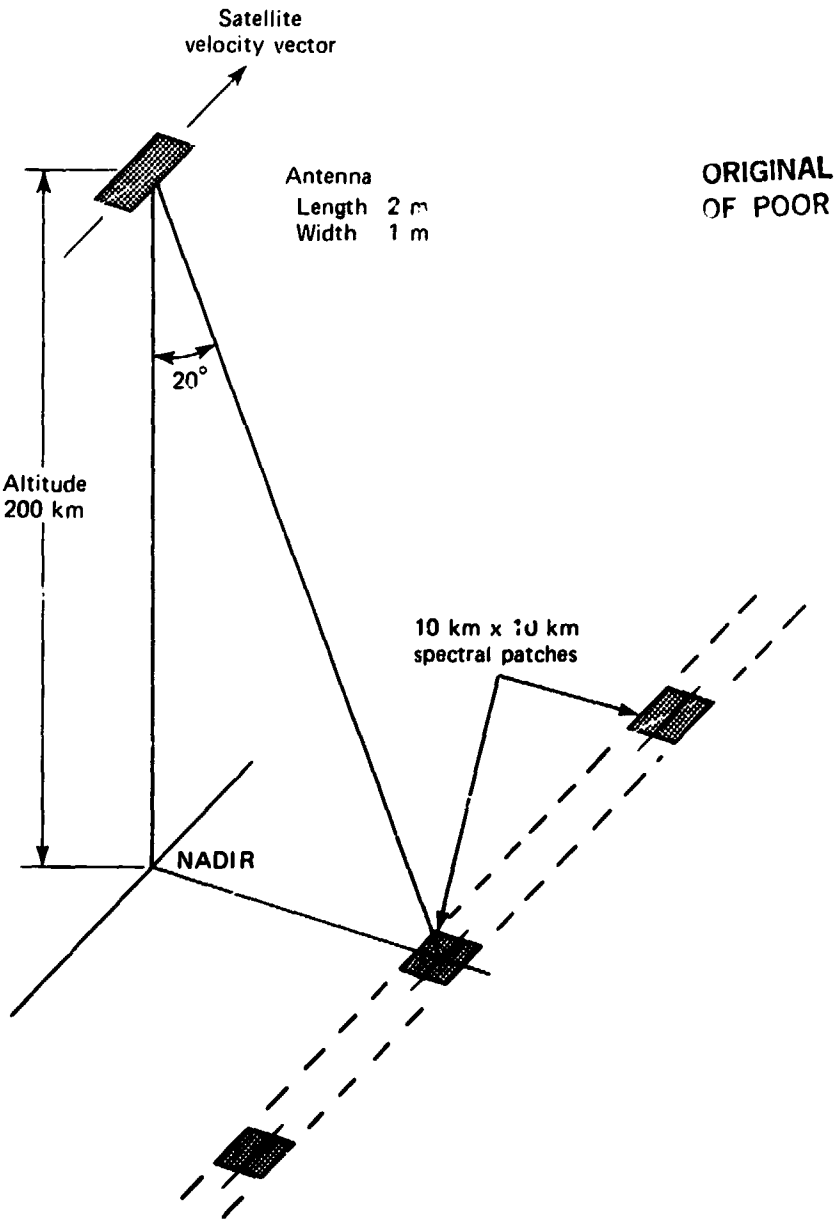

Fig. 5 Spectrasat basic configuration.

3.3 Some Questions to be Resolved

Determination of the major system characteristics of Spectrasat will naturally require a detailed design study. Of particular importance will be

1. the type and complexity of active drag compensation, necessary because of the very low altitude,

2. the required transmitter power, considering the smaller swath, smaller antenna, smaller range, the possibility of operating at a shorter wavelength (C-band), and the fact that substantial spectral and spatial averaging should be possible, and

3. the feasibility of on-board processing, given the smaller swath; the reduced azimuth compression ratio resulting from both the shorter transmitter wavelength and the possibility of presuming; and the insignificant range curvature resulting from the smaller swath.

Of equal importance is the question of Doppler smear, which in Seasat resulted in a lack of response to azimuth-travelling waves. Since theoretical models have not been very impressive in predicting the quality of SAR wave imagery, we should await the results of a decisive experiment, such as SIR-B, to verify that the lower altitude will indeed restore the necessary azimuth response.

Finally, it should be emphasized that many of the quantitative results summarized here are necessarily tentative, since they are based on an analysis of only one data set from Seasat. A comparable analysis of several data sets should be a prerequisite for extending the results more generally.

4. CONCLUSIONS

Analysis and interpretation of precision processed SAR wave imagery from Seasat over the past five years demonstrates a unique ability of SAR to monitor the large scale spatial evolution of the directional wave spectrum, directional properties of the wind field, and locations of current boundaries. Moreover, the geometry of Seasat (particularly its relatively high altitude and large swath) was not optimally chosen for the collection of global wave spectra. Many of the limitations of the Seasat SAR, therefore, were very likely not fundamental to the Doppler technique, but rather peculiar to the Seasat SAR parameters.

It is now appropriate to consider a dedicated SAR mission, not dictated by altimeter, scatterometer, or even SAR imagery requirements, but optimized solely for the acquisition of SAR ocean spectra. Such a system will be much simpler than Seasat, orbit at a much lower altitude, cover a much narrower swath, require less antenna area, consume less transmitted power, and permit an on-board, near-real-time processing capability.

Although such a mission should be unconstrained by other instrument requirements, it must nevertheless operate in the presence of a simultaneous altimeter and scatterometer mission. For only by synergistically combining the outputs of each of these sensors will we make significant progress in the global wave forecasting problem.

5. ACKNOWLEDGEMENTS

Results from the Seasat SAR analysis of Pass 1339, described in the first portion of this paper, are a collective effort of many of my colleagues at the Applied Physics Laboratory, particularly F. M. Monaldo, D. G. Tilley, T. W. Gerling, A. D. Goldfinger, and D. E. Irvine. We were also fortunate to have concurrent aircraft data supplied by D. B. Ross of the National Oceanic and Atmospheric Administration.

The Seasat SAR data analysis and interpretation is sponsored by the Office of Naval Research and the National Aeronautics and Space Administration. Conceptual design of Spectrasat is supported by Internal Research and Development funds.

6. REFERENCES

Beal, R.C., P.S. DeLeonibus and I. Katz (eds.): Spaceborne synthetic aperture radar for oceanography. The Johns Hopkins University Press, 1981, 215 pages.

Beal, R.C., D.G. Tilley and F.M. Monaldo, 1983: Large and small-scale spatial evolution of digitally processed ocean wave spectra from Seasat synthetic aperture radar. J. of Geophys. Res., Vol. 88, No. C3, pp. 1761-1778, February 28.

Fu, L.L. and B. Holt, 1982: Seasat views ocean and sea ice with synthetic aperture radar. Publication 81-120, Jet Propulsion Laboratory, Pasadena, California.

Series of papers on MARSEN. Journal of Geophysical Research, 1983, Vol. 88, pp. 9745-9882.

Sea Wave Modelling Project (SWAMP), (in press), Part I: Principal results and conclusions, from Wave Dynamics and Radio Probing of the Sea Surface, Miami, Florida, USA, ed. O.M. Phillips and K. Hasselmann.